

International Conference on Space Optics—ICSO 2022

Dubrovnik, Croatia

3–7 October 2022

Edited by Kyriaki Minoglou, Nikos Karafolas, and Bruno Cugny,



Update on the Ongoing ATHENA Optic Testing at PANTER



Update on the Ongoing ATHENA Optic Testing at PANTER

Vadim Burwitz*^a, Giuseppe Vacanti^b, Maximilien J. Collon^b, Nicolas Barrière^b, Marcos Bavdaz^c, Ivo Ferreira^c, Mark Ayre^c, Emily Tipper^b, Josef Eder^a, Elias Breunig^{a,d}, Gisela Hartner^a, Andreas Langmeier^a, Thomas Müller^a, Surangkana Rukdee^a, Thomas Schmidt^a

^aMax-Planck-Institut für extraterrestrische Physik, Giessenbachstr, 85748 Garching (Germany)

^bcosine, Warmonderweg 14, 2171 AH, Sassenheim, (The Netherlands)

^cESTEC, European Space Agency, Keplerlaan 1, 2201 AZ Noordwijk (The Netherlands)

^dBreunig Aerospace, St.-Georg Str. 3, 97199 Ochsenfurt (Germany)

ABSTRACT

At the PANTER X-ray test facility of the Max Planck Institute for Extraterrestrial Physics the testing of optics for ESAs ATHENA Mission is ongoing, as part of work towards the mission acceptance review. The ATHENA 2.6-m diameter mirror assembly comprises an aluminium support structure that holds the 600 Silicon Pore Optic Modules (SPOs) that focus the X-rays coming from the sources in the universe. At PANTER, these lightweight SPO modules are being tested individually or mounted in a petal that represents a sixth of the mirror structure. MM-0051 is the last iteration of a single mid-radius SPO to be tested at PANTER. A detailed description of the MM-0051 measurements is presented here. The characterization of three ATHENA “row 8” SPO optics produced to be inserted into the test petals shows that they will provide the necessary precision on the localization of the PSF on the detector to allow the verification of the thermal models of different mirror structure designs by the primes Airbus Defense and Space and Thales Alenia Space. Currently the opto-thermo-mechanical tests are ongoing at PANTER.

Keywords: X-ray optics, ATHENA, X-ray Astronomy, X-ray optics testing, PANTER

1. INTRODUCTION

ATHENA, ESAs large X-ray observatory mission, has been designed to study the Hot and Energetic Universe science theme [1]. The mission has a large 2.6 m diameter mirror made up of 600 Silicon Pore Optic (SPO) lenslets [2, 3]. It is planned to be launched in the mid 2030s. With the help of a hexapod support system the optic can focus the X-rays coming from cosmic objects onto one of two detectors. These detectors are a Wide Field Imager (WFI), a detector based on DEPFET technology [4] or an X-ray Integral Field Unit (X-IFU), a spatially resolving calorimeter [5]. The company *cosine* in the Netherlands is responsible for developing and producing the SPOs which make up the X-ray mirror [3]. Each SPO currently comprises two co-aligned X-ray optical units (XOUs) mounted between two invar brackets. In turn two High Performance Optic (HPO) stacks, each with the correspond to primary and secondary curvature, make up each XOU.

For more than 15 years the PANTER X-ray test facility [6] of the Max Planck Institute for Extraterrestrial Physics (MPE) located in the south west of Munich, Germany, has been involved in the development and testing of the SPO technology. Work on the 12 m focal length SPOs for the ATHENA Mission has been ongoing since 2015. With the X-ray source at distance of >120 m from the test optic the PANTER beamline allows the testing with a slightly divergent beam.

In this paper the results of the testing of the last mid-radius type SPO is presented. Furthermore, the results of the characterization of the three ATHENA “row-8” SPO mirror modules being used in the ongoing opto-thermo-mechanical tests for the ATHENA petal are also reported here.

* burwitz@mpe.mpg.de ; phone +49 89 30000-2415; <https://www.mpe.mpg.de>

2. TESTING SILICON PORE OPTICS AT PANTER

In June 2022 the SPO mirror module MM-0051 was tested at the PANTER X-ray test facility. The mirror module MM-0051 demonstrates characteristics of the middle radius region of the optic designed for the ATHENA telescope [7], although with a different rib pitch. The detailed specifications for this SPO optic are given in Table 1. The optics that will be mounted into the ATHENA petals that will undergo opto-thermo-mechanical tests at PANTER are the SPO mirror modules MM-0047, MM-0048 and MM-0049, and comply with the nominal Athena geometry. The specifications for these SPOs are listed in Table 4. The petals will allow the verification of the thermal models of different mirror structure designs by the primes Airbus Defense and Space and Thales Alenia Space. In Figure 1 left the optic holder supporting mirror modules MM-0047, 0048, 0049 on the top row and MM-0051 on the bottom is shown. A movable mask is used to select the optic that will be measured and also permit azimuthal scans to be performed. In Figure 1 right the mask installed on its translation stage can be seen behind the optics toward the X-ray source. All measurements at PANTER were made using the Al target (Al-K 1.485 keV) of the multi target electron impact source in conjunction with a 10 μm Al filter. One detector used is the TRoPIC pnCCD camera, with 256 x 256 pixels with each pixel 75 μm x 75 μm . The camera is read out 20 times a second and the electronics extracts the signal for the individual photon. Therefore, it is possible to obtain in an addition to the location on the detector, the energy of each photon. A second detector PIXI which is used in integration mode is a PI-MTE1300B camera with 1300 x 1340 pixels with each pixel 20 μm x 20 μm .

2.1 Test Setup

For the sake of efficiency, a holder supporting the MM-0051 optic and the ATHENA “row-8” MM-0047, MM-0048, and MM-0049 optics was manufactured so that it could be mounted on a hexapod on the extension optical bench in the PANTER 1-meter diameter beamline tube (see Figure 1). In Figure 2 a view of setup in the beamline tube is shown together with the coordinates system used for these optics in PANTER.



Figure 1. Photographs showing all four SPO mirror modules mounted in the holder as seen from the detector side. (left) In the image the mirror modules are labeled. (right) shows the final setup inside the PANTER beamline tube of the optics in their holder mounted on the hexapod which itself is mounted upon a translation stage. The movable mask for selecting the MM or XOU to be studied can be seen located behind the optic holder.

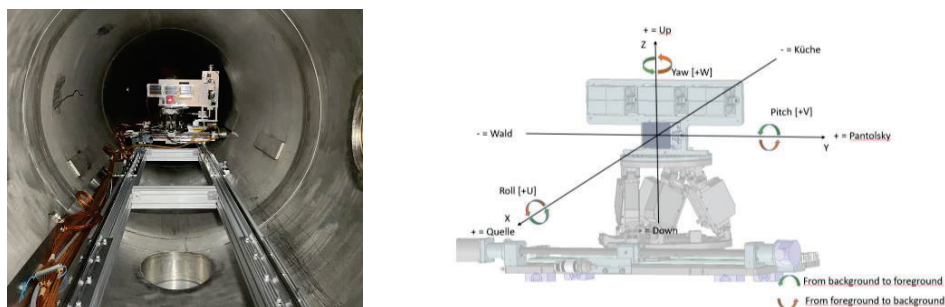


Figure 2. (left) Photograph of the optic mounted inside the chamber with MM-0051 centred behind the moveable mask. The view is looking towards the X-ray source. The alignment laser can be seen going through MM-0051. (right) depicts the coordinate system of the optics when mounted in PANTER.

3. MEASUREMENTS OF THE MID-RADIUS SPO MM-0051

The SPO mirror module MM-0051 is one of the best SPO mirror modules measured so far at PANTER. It is the result of a larger development effort concentrating not just on the optical performance but also on the manufacturing and handling processes associated with the making of hundreds such modules. The mirror module specs are given in Table 1. This single optic is mounted in the bottom row of the optic holder shown in the images in Figure 1.

Table 1. MM-0051 Specification

Parameter	Value	
	Inner radius XOU (iXOU)	Outer radius XOU (oXOU)
XOU names	XOU-0132	XOU-0131B
HPO name/s	HPO-2219 + HPO-2225	HPO-2230 + HPO-2223
Number of plates	34 + 1	34 + 1
Rib Pitch	1 mm	1 mm
Membrane Thickness	170 μ m	170 μ m
Azimuthal width	65.7 mm	65.7 mm
Radius R0 (plate 0) of the optic	709 mm	737 mm
Focal length	12000 mm	12000 mm

3.1 Alignment

Before the pump down of the vacuum chamber a pre-alignment in pitch and yaw of the optics was done using the alignment laser to ensure that the double reflection lands on the X-ray detector. The separation between the intersection plane of the optic and sensitive surface of the X-ray detector was set to the image distance of $i = 13336$ mm which corresponds to the nominal focal length of the optic of $f = 12000$ mm for a source to optic distance of $s = 119814$ mm at PANTER (for the divergent beam correction, the thin lens equation $1/f = 1/s + 1/i$ can be used).

Once the level of vacuum for operating the X-ray detector was reached first light images were taken to verify that the double reflection was in the expected position in X-rays using the 100% mask. Subsequently the position of the 100% mask was optimized and aligned with respect to the MM. In this 100% mask position a short focus search was performed followed by a pitch and yaw alignment of the complete mirror module (see Figure 3). The deviation from the laser pre-alignment is ~ 10 arcmin in pitch and ~ 1.3 arcmin in yaw.

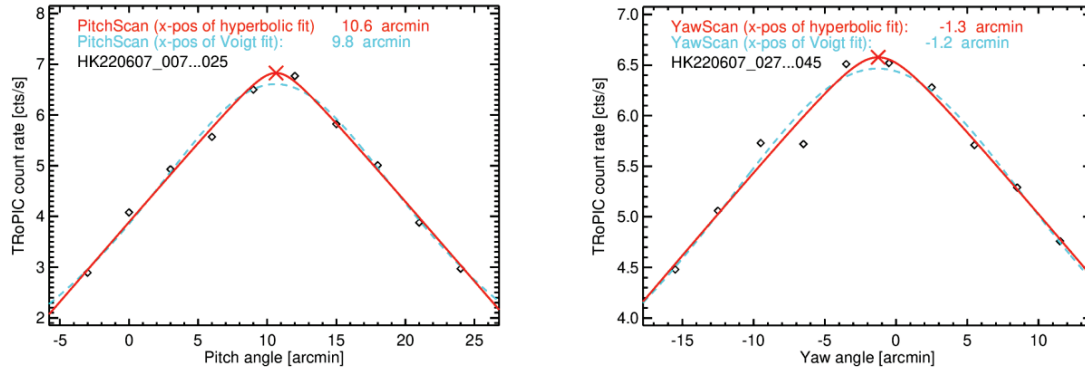


Figure 3. Shown are the pitch scan (left) and the yaw scan (right). Plotted are the data obtained using the 100% mask to illuminate the full MM with the TRoPIC camera at Al-K as well as the “best fit” hyperbola (red) and Voigt function (Cyan).

3.2 Focus Scan

After completing the pitch and yaw alignment of the mirror module MM-0051 a focus scan of the mirror module MM-0051, as well as for the individual X-ray optical units, the inner iXOU and outer oXOU was performed with the 100% mask in place. The results of the HEW and FWHM-X (the FWHM of the transverse PSF) fits of the focus search images are displayed in Figure 4. The focus searches were measured with both the TRoPIC and PIXI CCD cameras. The results of the best fits to the focus searches are summarized in Table 2 and Table 3.

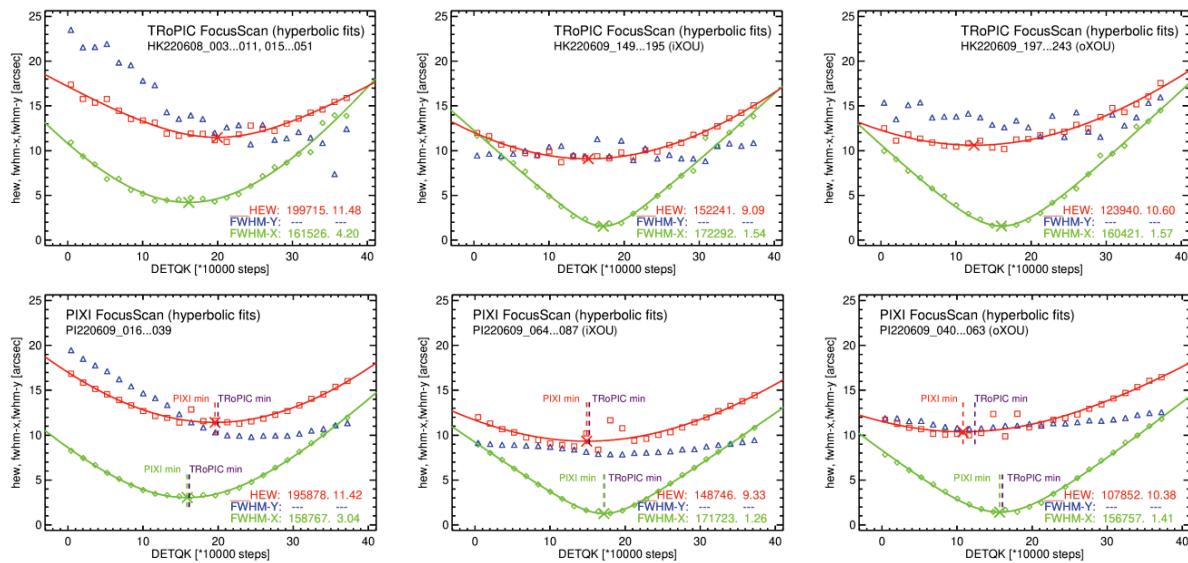


Figure 4 Shown in the top row are the measurements obtained with the TRoPIC CCD camera and in the bottom row the measurements obtained with PIXI CCD camera. The left column shows focus scans for the MM-0051 SPO, the central column the focus scans of the inner XOU-0132, and the right column the focus scans of the outer XOU-0131B. The scans are taken from -270 mm to +190 mm around image position corresponding to the nominal 12 m focus. Shown are the best hyperbola fits to the HEW points (red) and to the FWHM-X points (green). The FWHM-Y points are shown for completeness but are not fitted. The results are given in steps (1 step corresponds to 1.25 μm) and arcsec.

Table 2 Summary of all best focus positions from focus searches with TRoPIC of MM, iXOU, oXOU with 100% mask at Al-K. The best fit values for the focus position are given in steps, the HEW and FWHM-X values in arcseconds.

Focus search TRoPIC 100% Mask	Relative Position* (mm)	Detector QK (steps)	HEW (arcsec)	FWHM-X (arcsec)	Best Focus Type (referred as ...)
MM-0051 (MM)	-25.6	199715	11.5	---	HEW (TRoPIC)
	-73.3	161526	---	4.2	FWHM-X (TRoPIC)
inner XOU-0132 (iXOU)	-84.8	152241	9.1	---	iHEW (TRoPIC)
	-59.9	172292	---	1.5	iFWHM-X (TRoPIC)
outer XOU-0131B (oXOU)	-120.3	123940	10.5	---	oHEW (TRoPIC)
	-74.7	160421	---	1.6	oFWHM-X (TRoPIC)

*Relative position is the position relative to the laser position (nominal 12 m focus at infinity).

Table 3 Summary of all best focus positions from focus searches with PIXI of MM, iXOU, oXOU with 100% mask at Al-K. The best fit values for the focus position are given in steps, the HEW and FWHM-X values in arcseconds.

Focus Search PIXI 100% mask	Relative Position* (mm)	Detector QK (steps)	HEW (arcsec)	FWHM-X (arcsec)	Best Focus Type (referred as ...)
MM-0051 (MM)	-31.2	195878	11.4	---	HEW (PIXI)
	-77.6	158767	---	3.0	FWHM-X (PIXI)
inner XOU-0132 (iXOU)	-90.1	148746	9.3	---	iHEW (PIXI)
	-61.4	171723	---	1.3	iFWHM-X (PIXI)
outer XOU-0131B (oXOU)	-141.2	107852	10.4	---	oHEW (PIXI)
	-80.1	156757	---	1.4	oFWHM-X (PIXI)

*Relative position is the position relative to the laser position (nominal 12 m focus at infinity).

3.3 Deep on-axis PSFs in best focus positions

Using the best focus positions determined in Section 3.2 for the MM-0051 mirror module, the iXOU and oXOU deep PSF exposures obtained using both TRoPIC and PIXI (see summaries in Table 4 and Table 5) were obtained at the so-called laser position, the image distance of $i = 13336$ mm that corresponds to at the nominal design focal length of $f = 12000$ mm. Then at the best HEW position for the MM and the individual XOU's. Finally, the PSFs were obtained at the best transverse PSF (FWHM-X) positions, these are important for the spectral resolution of the Arcus mission [8]. In Table 4 the HEW, FWHM-X values of the PSFs measured in the (laser) position are shown together with the corresponding images. For the Mirror Module (both XOU's), the inner iXOU and the outer oXOU with 100% mask (full illumination) we obtain HEWs of 11.4 arcsec, 9.6 arcsec and 11.9 arcsec respectively, these numbers are given for the nominal focal length (Table 4). In the measured best HEW focus position of the MM, the iHEW and oHEW focus positions of the iXOU and oXOU the measured HEWs are 11.5 arcsec, 9.3 arcsec, and 10.5 arcsec as measured with TRoPIC (Table 5).

Looking at the 100% mask results, the two XOU's do not yet place their PSF at the same location in the focal plane, in this case the distance between the two PSFs is just under 180 μm at the nominal focal distance of 12 m: although this is the best result obtained so far, further work is being done to reduce this difference, so that the performance of each individual XOU contributes optimally to the performance of the MM.

Table 4 Overview of the deep on-axis PSFs imaged with TRoPIC at the image distance corresponding to the nominal 12-m design focus positions at Al-K for the MM, the iXOU, and the oXOU. The mask used and the HEW, and transverse PSF FWHM-X are displayed together with the image of the corresponding PSF. Images and data correspond to the laser position measurements in Table 5, where we also report values obtained during the characterization at the BESSY II synchrotron facility (1 keV).

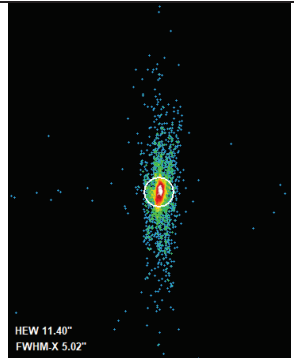
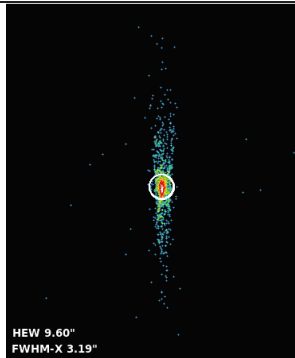
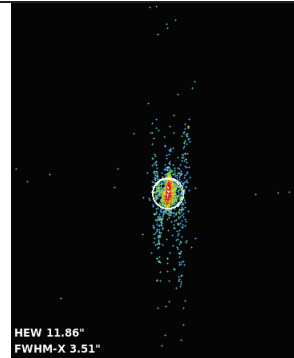
Optic	MM	iXOU	oXOU
HEW (arcsec)	11.4	9.6	11.9
FWHM-X (arcsec)	5.0	3.2	3.5
TRoPIC PSF Images			

Table 5 Summary of all deep TRoPIC images of the MM, iXOU, oXOU with 100% mask at Al-K. Also shown, where available, the results obtained at the BESSY II synchrotron (1 keV).

Deep Images TRoPIC 100% Mask	Relative Position* (mm)	Detector QK (steps)	HEW (arcsec)	BESSY HEW (arcsec)	FWHM-X (arcsec)	Best Focus Type (referred as ...)
MM-0051 (MM)	0.0	220200	11.4	n/a	5.0	Laser
	-25.6	199715	11.5	n/a	4.5	HEW (TRoPIC)
	-73.3	161526	11.6	n/a	4.4	FWHM-X (TRoPIC)
inner XOU-0132 (iXOU)	0.0	220200	9.6	9.4	3.2	Laser
	-84.8	152241	9.3	9.3	2.1	iHEW (TRoPIC)
	-59.9	172292	8.7	n/a	1.7	iFWHM-X (TRoPIC)
outer XOU-0131B (oXOU)	0.0	220200	11.9	11.2	3.5	Laser
	-120.3	123940	10.5	10.2	2.6	oHEW (TRoPIC)
	-74.7	160421	9.8	n/a.	1.8	oFWHM-X (TRoPIC)

*Relative position is the position relative to the laser position (nominal 12 m focus at infinity).

3.4 Azimuthal (Hartmann) scan

During this scan a 3 mm wide mask is shifted across the inner and outer XOU's in order to monitor the quality of the PSF with respect to the azimuthal position. This method provides detailed knowledge on where errors in the optic mainly come from. A compilation of the images made at each azimuth position during the scan is displayed in Figure 5 and the HEW results obtained from the analysis of these PSFs are shown in Figure 6. Once again there is an excellent agreement between the measurements taken at PANTER and those taken at the XPBF 2 [9], showing that the assembly and characterization of a SPO using a pencil beam [10] is a reliable technique for the assembly and characterization of segmented X-ray optics. Figure 5 shows the images of the optics taken during the azimuthal scan. This ‘‘Hartmann test’’ indicates that the performance is better than 8’’ over more than 70% of the optic, and that the degradation of the sides is significantly reduced with respect to earlier samples. The numbers computed for the smaller regions around the center of the optic are summarized in Table 6. The iXOU was scanned in the focus position 152881 steps and the oXOU in the focus position 124580 steps, in the best TRoPIC iHEW and oHEW positions.

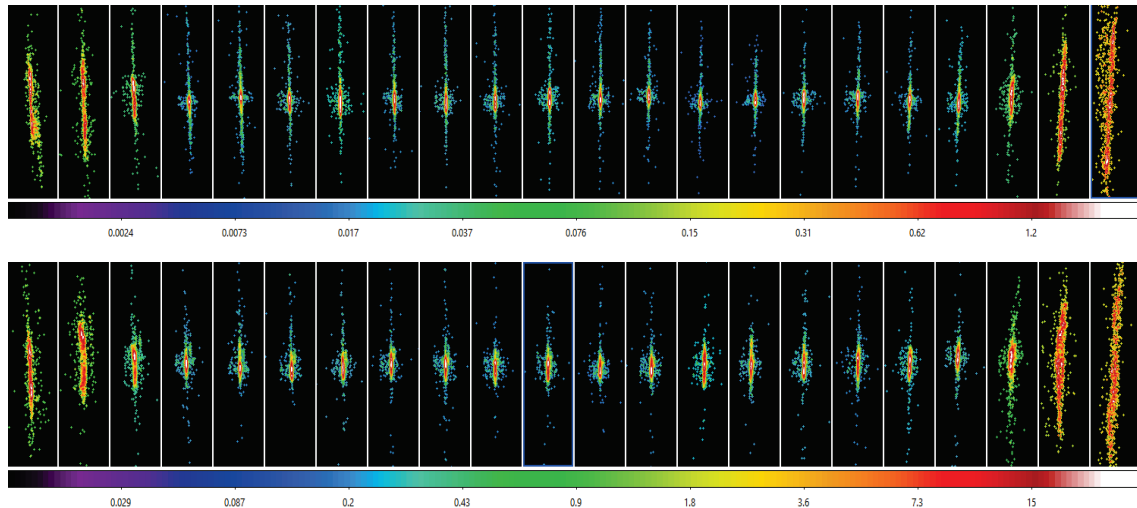


Figure 5. Compilation of images obtained during the azimuthal scans of the inner XOU (top) and outer XOU (bottom) with 3 mm mask, the scan runs horizontally from the left side to the right side of the XOU's. In Figure 6 the analysis of the above PSFs is shown.

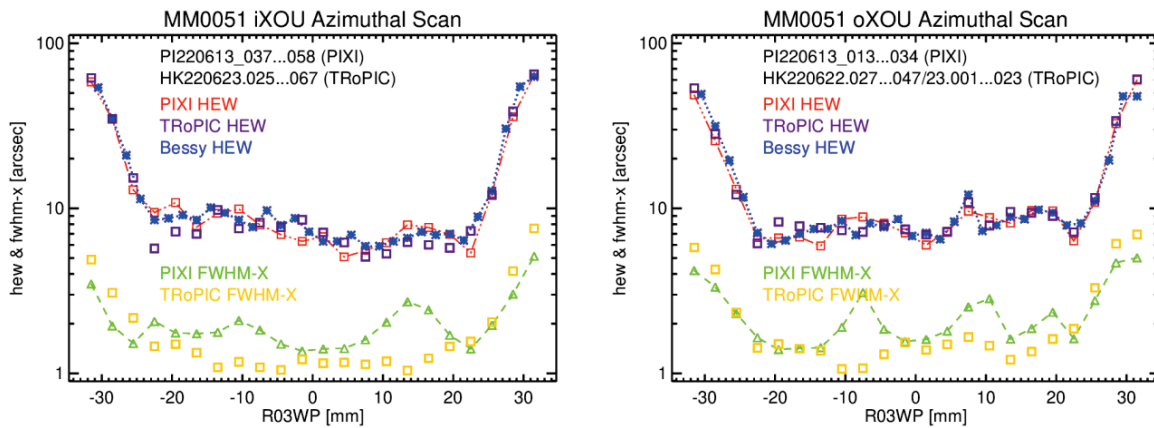


Figure 6. Overview of the azimuthal scan results obtained using the PANTER TRoPIC (purple & yellow data points) and PIXI (red & green data points) detectors. The graphs show the results of the azimuthal scans with the 3 mm slit mask over (left) the inner XOU-0132 (iXOU) and (right) the outer XOU-0131B (oXOU). For comparison, the results obtained at BESSY are overlaid with a dotted blue line with ‘*’ symbols at the 22 azimuth positions.

Table 6 Here using the azimuthal scan PSF images taken with PIXI, summed up images have been created and analysed to obtain the HEW and the FWHM-X values for different sized azimuthal regions of the optic. All selected regions are centered on the middle of the optic. The 70% values obtained at BESSY are shown in parenthesis.

XOU	iXOU		oXOU	
Percentage of XOU	HEW (arcsec)	FWHM-X (arcsec)	HEW (arcsec)	FWHM-X (arcsec)
100%	10.5	2.1	10.4	2.3
91%	8.9	2.1	9.3	2.3
82%	7.7	2.1	8.3	2.3
73%	7.3 (7.6)	2.1	7.8 (8.3)	2.2

3.5 Effective Area

When computing the expected effective area for MM-0051 SPO one has to keep in mind that the optic is uncoated and therefore the surface reflectivity is that of SiO₂. In Table 7 we show the measured effective areas for the MM and each XOU, together with the highest possible predicted effective area, assuming ideal XOUs. Pending more detailed modelling we take that the ideal effective area must be reduced by 10% to account for the alignment and manufacturing obscuration factors.

Table 7. Results of the effective area measurements at Al-K for the MM-0051, as well as for the inner and outer XOUs with the 100% mask in place.

Mask	Module	Predicted Effective Area (cm ²)	Predicted Effective Area -10% (cm ²)	Measured Effective Area (cm ²)	1 σ error Effective Area (cm ²)
100%	MM	15.3	13.8	13.2	0.5
	Inner XOU	7.5	6.7	6.7	0.4
	Outer XOU	7.8	7.0	6.3	0.4

3.6 Vignetting curves

The data for the vignetting curves was obtained by stepping (4 arcmin steps) through a sequence of off-axis tilt (pitch) and rotation (yaw) angles which correspond to different off-axis positions. The curves displayed in Figure 7 and Figure 8 show the dependence of the effective area of the optic as a function of the pitch and yaw angles for both the inner and outer XOUs.

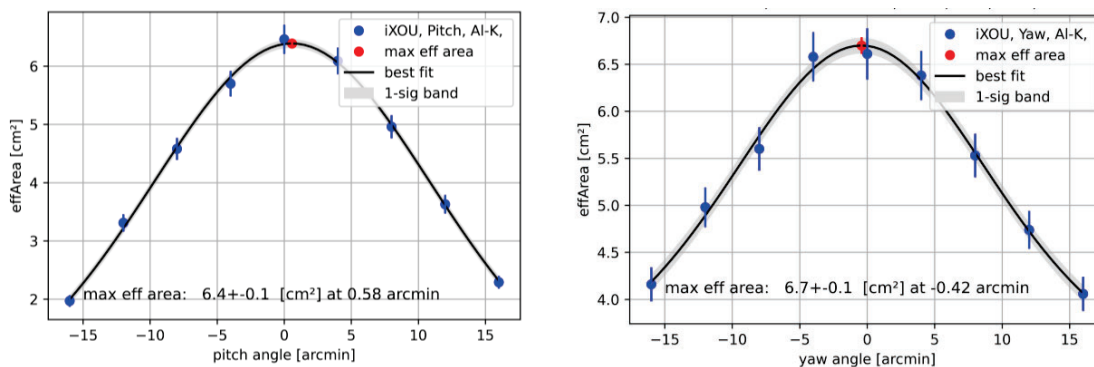


Figure 7 (left) Pitch and (right) Yaw scans of effective area vignetting curve of the iXOU

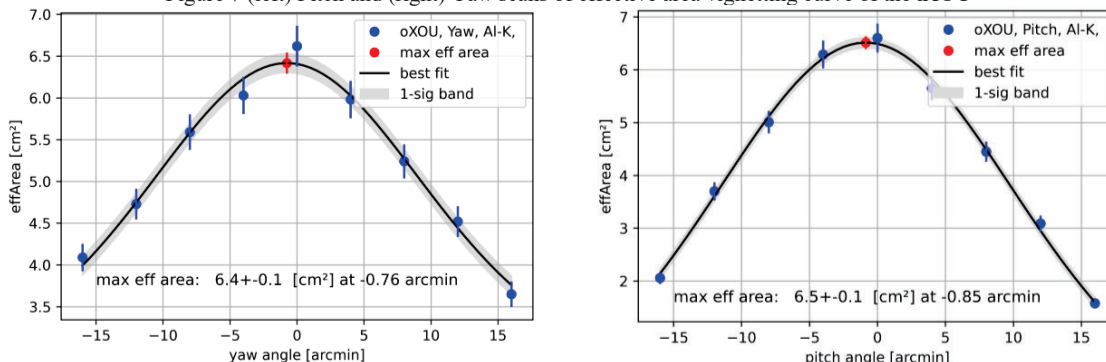


Figure 8 (left) Pitch and (right) Yaw scans of effective area vignetting curve of the oXOU

3.7 MM-0051 Measurements Summary

The MM-0051 optic is also one of the best measured mirror modules so far in full illumination. With 100% mask (full illumination) we obtain a HEWs of 11.4 arcsec, 9.6 arcsec and 11.9 arcsec respectively for the Mirror Module (both XOUs), the inner iXOU and the outer oXOU. These numbers are given for the nominal focal length. A 70% mask was not available but we are able to determine the PSF for the inner 70% of the optic by adding up the images from that region obtained during the azimuthal scan of the iXOU and oXOU. These summed images yield a HEW of 7.2 arcsec and 7.8 arcsec for the iXOU and oXOU. These values were obtained in the corresponding best HEW focus positions for each XOU.

The confocality of the system has been improved substantially, but it needs to be improved further to convert the performance of the individual XOUs into a comparable aggregate MM performance.

The effective areas measured, both at XOU and MM level, are compatible with expectations.

4. MEASUREMENTS OF ATHENA ROW8 SPOS MM-0047, MM-0048, AND MM-0049

These three mirror modules described here were tested in preparation, of the ATHENA petal opto-thermo-mechanical tests that will follow after this campaign. The details of the optics are summarized in Table 8. These are three prototype flight design ATHENA “row-8” type modules with a larger 2.3 mm rib pitch and thinner 110 μm membrane. As the plates used for assembling the stacks for these XOUs are not wedged only the central plates 19 are aligned to focus at ATHENA’s nominal 12 m focal length. To ensure that only light from the plates 19 of XOU in MMs is focused on the detector a fixed mask with slit with a width corresponding to 70% of the width of the stack and one plate high was installed on each primary stack of the XOUs. These optics can be seen populating the top row of the optics holder shown in the images in Figure 1. The three SPO optics were fully characterised using the PIXI X-ray detector, as this will be the camera used during the ATHENA petal opto-thermo-mechanical tests see Section 4.1.

Table 8 Specifications of MM-0047, 0048, 0049

Parameter	Value		
	Full Module	Inner XOU (iXOU)	Outer XOU (oXOU)
XOU names	MM-0047	XOU-0117	XOU-0118
	MM-0048	XOU-0122	XOU-0121
	MM-0049	XOU-0124	XOU-0125
Number of plates		37 + 1	37 + 1
Rib Pitch		2.3 mm	2.3 mm
Membrane thickness		110 μ m	110 μ m
Azimuthal width of the XOU		86.1 mm	86.1 mm
Radii of the XOUs (mm)		R0 (plate 0) 753.2 R19 (central plate 19) 737.6	R0 (plate 0) 783.2 R19 (central plate 19) 767.7
Focal length		12000 mm	12000 mm

The quality of these three prototype optics is good enough for allowing us to track the location of the PSF with an accuracy of better than 5 μ m on the detector during the opto-thermo-mechanical test campaign that is currently ongoing at PANTER.

4.1 ATHENA petal opto-thermo-mechanical tests at PANTER

Currently tests are ongoing at PANTER in which MPE, ESA, cosine and Media Lario are performing two complex opto-thermo-mechanical tests of the two full scale 1/6th sectors of the final ATHENA mirror assembly structure produced by the potential ATHENA primes Airbus Defense and Space (ADS) and Thales Alenia Space (TAS). For these tests a set of 3 ATHENA row-8 SPO MMs have been produced following the flight configuration recipe. The characterisation of these optics prior to incorporating them into the optics in the ATHENA petals is described in Section 4. The SPO MMs will be mounted into each sector by Media Lario at PANTER shortly before each test begins. After the first petal test Media Lario will remove the optics from the first tested petal so that they can be reused in the second petal.

The setup of the opto-thermo-mechanical tests in the vacuum chamber is shown in Figure 9 together an image of the setup as mounted in the chamber. Frames have been manufactured to hold the shrouds on the space side and the spacecraft side as well as a kinematic mount for holding the petals during the test. As these frames are large and heavy (about 380 kg including the Petals) they have to be mounted on the movable optical bench (tilt and rotation movement of up to $\pm 3^\circ$) in the large vacuum chamber. As the image distance is about 13.3 m from the optics the image is formed outside the large chamber. A smaller 3-m long extension chamber containing a 3-axis translation stage for the CCD camera can be attached to the main chamber via a DN250 flange. This requires a very precise positioning of the illuminated optics in the petal to ensure the focused images make it to the detectors. A gap between the shrouds both on the hot and cold side of the setup allows the X-ray to illuminate the optics and the reflected X-rays to form an image, the PSF, on the detector.

The main goal of these petal tests is to quantify the impact thermal gradients on the thermoelastic behavior of the sectors and compare the measurements with the model predictions. During these tests the location of the centroids of the 3 X-ray PSFs of the ATHENA “row-8” optics mounted in the petal will be monitored as a function of the thermal load cases listed in Table 9.

The heaters and thermocouples were installed on the petal to ensure that together with the PANTER cooling and heating shrouds the required gradients can be generated and measured on the petals. For this in the most extreme case the cold shrouds will be cooled to -40°C and warm ones heated to $+35^\circ\text{C}$. Furthermore, heaters installed on the petal close to the optics will allow an even larger enhancement of the load case gradients.

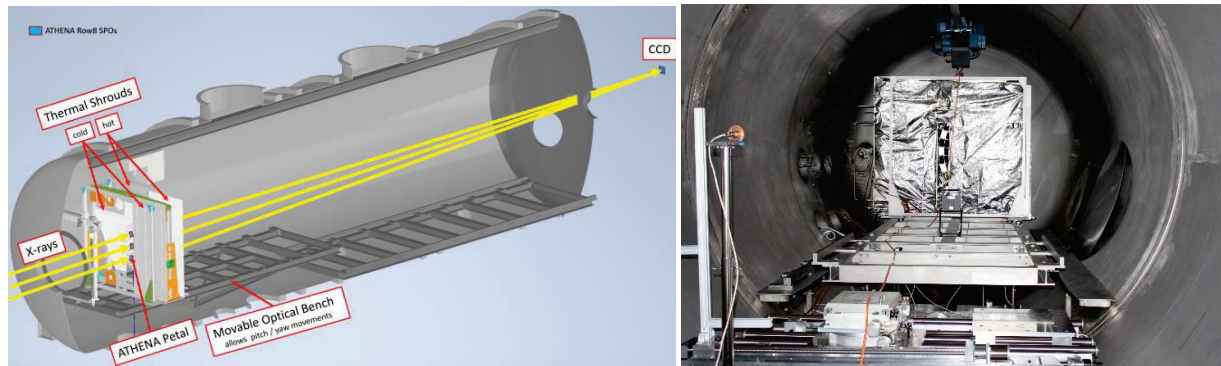


Figure 9. (left) Overview of the thermal opto-thermo-mechanical test of the ATHENA petals that is due to take place in summer 2022 at PANTER. From the left the X-rays form the X-ray source enter the three ATHENA “row-8” optics that are mounted in the petal and are double reflected on to the detector which is mounted on an x-y-z-stage in an extension chamber (not shown) attached to the large PANTER vacuum chamber. (right) picture of the PANTER vacuum chamber with the shroud around the petal wrapped in multilayer insulation. The shroud is mounted on the movable optical bench that enables pitch and yaw movements of the setup. The three optics (top MM-0049, center MM-0048, bottom MM-0047) mounted in the petal are visible, with the setups as mounted in the vacuum chamber prior to testing the X-ray come from the rear side of the setup.

Table 9. Summary of the load cases for testing the ATHENA petals at PANTER. The direction -Z is towards the X-ray source.

Load Case	0	2	1	3	4	1B	5	6	0B
Description	Initial ‘blank’ test, petal at 20°C	2.5°C thermal gradient in Z direction	5°C thermal gradient in Z direction	thermal gradient in Y direction 1	thermal gradient in Y direction 2	5°C thermal gradient in Z direction	Cold shroud environment, petal at 10°C	Warm shroud environment, petal at 15°C	Final ‘blank’ test, petal at 20°C
Chamber Temp. (°C)	+20	+20	+20	+20	+20	+20	+20	+20	+20
+Z Shroud Temp. (°C)	+20	+35	+25	+5	+5	+5	+5	+15	+20
-Z Shroud Temp. (°C) Wald/Pantolsky	+20 / +20	-40 / -33	-40 / -32	-43 / -38	-43 / -37	-43 / -36	+5	+15	+20
Heater Group 1 (W)	0	2.5	7.0	7.0	0	7.0	0	0	0
Heater Group 2 (W)	0	2.5	7.0	3.5	3.5	7.0	0	0	0
Heater Group 3 (W)	0	2.5	7.0	0	7.0	7.0	0	0	0

5. SUMMARY

The silicon pore optic mirror module MM-0051 underwent rigorous X-ray testing at PANTER. The results obtained are commensurate with those obtained at BESSY. We find that the XOUs of MM-0051 have in their best focus have HEWs over the 100% of the XOU a HEW of 10.5" and a HEW better than 8" arcsec over the inner 70-80% of the optic. These XOUs represent the current state of the art in optical quality that can be achieved prior to the introduction of the new ATHENA geometry with wider 2.3 mm rib spacing and thinner membranes 110 μm and of the new ion beam figuring of wafers to improve on the plate wedge.

The ATHENA petal opto-thermo-mechanical test at PANTER are currently ongoing proceeding nominally and will be completed in September 2022. The tests will yield insight into how well modelling represents the real Mirror Assembly Module Demonstrator (MAMD) petals.

ACKNOWLEDGEMENTS

The work performed at the PANTER X-ray test facility has in part been supported by the European Union's Horizon 2020 Program under the AHEAD2020 project (grant agreement n. 871158)

REFERENCES

- [1] Nandra, K., et al., "The Hot and Energetic Universe: A White Paper presenting the science theme motivating the Athena+ mission," [arXiv:1306.2307](https://arxiv.org/abs/1306.2307) (June 2013)
- [2] Bavdaz, M. et al., "ATHENA x-ray optics development and accommodation," Proc. SPIE 11822, Optics for EUV, X-Ray, and Gamma-Ray Astronomy X, 1182205 (23 August 2021); doi: 10.1117/12.2594689
- [3] Collon, M. J., et al., "Silicon pore optics x-ray mirror development for the Athena telescope," Proc. SPIE 11822, Optics for EUV, X-Ray, and Gamma-Ray Astronomy X, 1182206 (31 August 2021); doi: 10.1117/12.2593505
- [4] Meidinger, N. et al, "The Wide Field Imager instrument for Athena," Proc. SPIE 10397, UV, X-Ray, and Gamma-Ray Space Instrumentation for Astronomy XX, 103970V (29 August 2017); doi:10.1117/12.2271844
- [5] Barret, D. et al, "The ATHENA X-ray Integral Field Unit (X-IFU)," Proc. SPIE 10699, Space Telescopes and Instrumentation 2018: Ultraviolet to Gamma Ray, 106991G (31 July 2018); doi: 10.1117/12.2312409
- [6] Burwitz, V., R. Willingale, C. Pellicciari, G. Hartner, M.-M. La Caria, "Testing and calibrating the ATHENA optics at PANTER," Proc. SPIE 10399, Optics for EUV, X-Ray, and Gamma-Ray Astronomy VIII, 103990O (13 October 2017); doi: 10.1117/12.2274237
- [7] Barrière, N. M., Bavdaz, M., Collon, M. J., et al. "Silicon Pore Optics", arXiv:2206.11291 (2022)
- [8] Smith, R. K. "The Arcus soft x-ray grating spectrometer explorer," Proc. SPIE 11444, Space Telescopes and Instrumentation 2020: Ultraviolet to Gamma Ray, 114442C (22 December 2020); doi: 10.1117/12.2576047
- [9] Krumrey, M., et al., "New x-ray parallel beam facility XPBF 2.0 for the characterization of silicon pore optics", Proc. SPIE 9905, Space Telescopes and Instrumentation 2016: Ultraviolet to Gamma Ray, 99055N (11 July 2016); doi:10.1117/12.2231687
- [10] Vacanti, G., Barrière, N., Bavdaz, et al. "Measuring silicon pore optics", Proc. SPIE 10399, Optics for EUV, X-Ray, and Gamma-Ray Astronomy VIII, 103990N (8 September 2017); doi: 10.1117/12.2274357